

Civil engineering  
Statybos inžinerija

**COMPARATIVE ANALYSIS OF FLEXURAL STIFFNESS OF  
CONCRETE ELEMENTS WITH DIFFERENT TYPES OF COMPOSITE  
REINFORCEMENT SYSTEMS**

Haji Akbar SULTANI <sup>1\*</sup>, Viktor GRIBNIAK <sup>1</sup>, Arvydas RIMKUS <sup>1</sup>,  
Aleksandr SOKOLOV <sup>1</sup>, Lluís TORRES <sup>2</sup>

<sup>1</sup>*Vilnius Gediminas Technical University, Vilnius, Lithuania*

<sup>2</sup>*University of Girona, Girona, Spain*

Received 05 June 2020; accepted 09 October 2020

**Abstract.** Various materials and reinforcement technologies have been created for concrete structures. However, there is no uniform methodology to compare the mechanical characteristics of different reinforcement systems. In structural systems, residual stiffness can estimate the efficiency of the reinforcement. This study introduces a simplified approach for the flexural stiffness analysis. It employs a new testing layout designed with the purpose to form multiple cracks in a small laboratory specimen. The achieved solution requires neither iterative calculations nor a description of the loading history. Several composite reinforcement schemes, including internal glass fibre reinforced polymer (GFRP) bars, carbon fibre reinforced polymer (CFRP) sheets and near-surface mounted (NSM) strips are considered. The analysis of the test results reveals a substantial efficiency of the external CFRP reinforcement systems.

**Keywords:** concrete composite, reinforcement, residual stiffness, analytical model, flexural tests.

## Introduction

Various materials and reinforcement technologies have been created for concrete structures, but there is no uniform methodology to compare the mechanical characteristics of different reinforcement systems. Residual stiffness of flexural elements is the focus of the research. Numerous studies investigated this issue. However, only several works addressed flexural effects. Fundamental studies by Kaklauskas and Ghaboussi (2001) and Torres et al. (2004) could be mentioned in this context. Elaborate numerical procedures are an intrinsic attribute of the “exact” approaches (Gribniak et al., 2017). Iterative nature of the analysis procedures often complicates applicability of the exact techniques: the calculation errors are accumulated following the load history (Gribniak et al., 2017). The development of more reliable algorithms employed the reinforcement-related tension-stiffening concept was the consequence of the further improvements (Kaklauskas et al., 2011; Torres et al., 2015; Kaklauskas & Gribniak, 2016). Such models, however, are not useful for the analysis of the elements reinforced with a combination of different types of composite reinforcement.

Residual stiffness can determine the efficiency of the reinforcement system (Gribniak et al., 2019). That is the object of this research. A new testing procedure was developed to estimate residual flexural stiffness of the concrete elements with composite reinforcement systems. Several composite reinforcement schemes including internal glass fibre reinforced polymer (GFRP) bars, external bond reinforcement (EBR) system using carbon fibre reinforced polymer (CFRP) sheets, and near-surface mounted (NSM) strips are considered. The proposed geometry of the test specimens is suitable for application of the tension-stiffening modelling concept (related to average deformations of the concrete). The corresponding analytical model can represent stress-strain behaviour of tensile concrete (independently on the reinforcement system applied). The equivalent tensile stress of the concrete is the parameter proposed to quantify the residual stiffness of the flexural element. Representing a closed-form solution of the flexural stiffness problem, the proposed analytical model requires neither iterative calculations nor a description of the loading history. The application of this technique is illustrated experimentally.

\*Corresponding author. E-mail: [haji-akbar.sulatani@vgtu.lt](mailto:haji-akbar.sulatani@vgtu.lt)

### 1. Research object and objectives

The slab-shaped beam specimens have an identical rectangular cross-section of the concrete that was reinforced with internal bars, NSM CFRP strips, or EBR using CFRP sheets. The testing layout is designed with the purpose to form multiple cracks in a small laboratory specimen. The geometry of specimens was chosen using the trial-and-error iterative procedure. The satisfaction of the simplified modelling assumption (rectangular distribution of stresses in the tensile concrete) was used as the design criterion. In other words, the “exact” tension-stiffening diagram (Gribniak et al., 2017) had to have the shape as close as possible to rectangular.

This study employs 16 flexural specimens. Table 1 defines the main parameters of the beams. In this table,  $h$ ,  $b$ , and  $d$  are the height, width, and effective depth of the

cross-section;  $A_r$  and  $E_r$  are the area and elasticity modulus of the reinforcement, respectively. The table also defines the compressive strength of the  $\varnothing 150 \times 300$  mm concrete cylinder at 28 days ( $f_{c,28}$ ) and age ( $t$ ) of testing ( $f_{cm}$ ). The first letter in the notation of the beams describes the reinforcement type (“G” = internal GFRP bars, “N” = NSM CFRP strips, and “C” = EBR CFRP sheets); the numerals split the specimens having identical reinforcement scheme. The cross-sections of the beams can be found in Figure 1.

The experimental beams were cast using steel forms and removed from the moulds in the age of 2–3 days. The ordinary concrete specimens were cured at an average relative humidity of 73% and a temperature of 20 °C. The NSM system and EBR sheets were attached to the dry concrete specimens before the tests. The beams reinforced with internal bars were stored in water until the testing day to reduce the shrinkage effect.

Table 1. Main parameters of the beam specimens

Specimen	$h$ , mm	$b$ , mm	$d_1$ , mm	$A_{r1}$ , mm <sup>2</sup>	$E_{r1}$ , GPa	$f'_c$ , MPa	$t$ , days	$f_{cm}$ , MPa
G1	101	199	75	15.08	64.4	46.61	31	46.04
G2	101	200	76	15.08	64.4	46.61	31	46.04
G3 <sub>w</sub>	100	200	75	15.08	64.4	49.69	39	46.04
G4 <sub>w</sub>	103	198	83	15.08	64.4	49.69	39	46.04
N1	104	200	94	28	170	49.56	62	44.34
N2	105	197	95	28	170	50.70	62	43.02
N3 <sub>w</sub>	102	198	92	28	170	50.70	63	43.02
N4 <sub>w</sub>	106	199	80	28	170	50.70	63	43.02
C1	110	204	110	23.2	230	46.61	31	46.04
C2	104	196	104	23.2	230	46.61	31	46.04
C3 <sub>w</sub>	99	202	101	23.2	230	49.69	39	46.04
C4 <sub>w</sub>	113	195	109	23.2	230	49.69	39	46.04
C5	102	199	103	23.2	230	50.69	48	44.95
C6	103	199	104	23.2	230	50.69	47	44.95
C7	104	200	105	23.2	230	49.56	48	44.34
C8	104	199	104	23.2	230	50.69	48	44.95

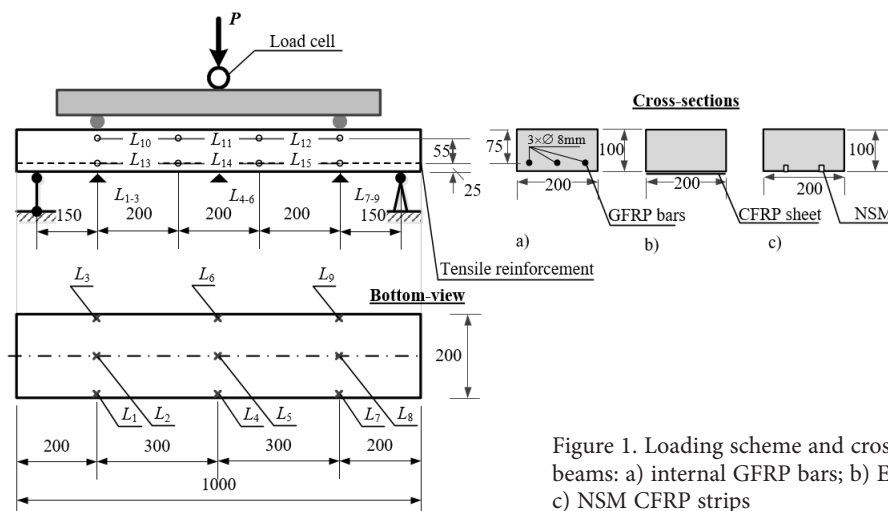


Figure 1. Loading scheme and cross-sections of the beams: a) internal GFRP bars; b) EBR CFRP sheets; c) NSM CFRP strips

## 2. Beam tests

The 1000 mm long specimen is tested under a four-point-bending scheme with 600 mm pure bending zone and two 150 mm shear spans. The specimens were produced in several batches using the same concrete compositions. The composition of the concrete (for one cubic meter) is following: 356 kg of cement CEM I 42.5 R, 163 l of water, 177 kg of limestone powder, 890 kg of 0/4 mm sand, and 801 kg of 4/16 mm crushed aggregates; 1.97% (by the cement weight) of the superplasticizer *Mapei Dynamon XTend* and 3.5 kg of the admixture *SCP 1000 Optimizer*. The beams were reinforced with 8 mm GFRP bars, EBR with CFRP sheets, or NSM CFRP strips (Figure 1). The previous study (Gribniak et al., 2019) indicated the insufficient resistance of FRP composites to shear loads. In this study, six beams had CFRP wrapping in the shear zones to avoid premature failure of the specimens. The subscript “w” designates these samples in Table 1. The same unidirectional *MapeWrap C UNI-AX* CFRP sheets were used as external and shear reinforcement. The equivalent thickness of the dry material was 0.166 mm.

As shown in Figure 1, the surface deformations were assessed using linear variable displacement transducers (LVDT)  $L_{10}$ – $L_{15}$  attached in two continuous lines to side surface of the specimen. The vertical displacements in pure bending zone were measured by nine LVDT ( $L_1$ – $L_9$ ,

Figure 1). The data logger ALMEMO 5690-2 collected the output results of all LVDT and the load cell.

Deformations and crack pattern of the side surface of the specimen were fixed with the help of digital image correlation system (DIC). Two cameras IMAGER E-LITE 5M were used for this purpose. The cameras were placed on a tripod at the 3.0 m distance from the specimens; the gap between the cameras was equal to 0.4 m. The cameras, incorporating a charge-coupled device (CCD) detector, have a resolution of 2456×2085 pixel at the 12.2 fps rate. Figure 2 demonstrates the evolution of the cracks identified by the DIC system. The numbers in circles highlights the cracking sequence; the arrows indicate the load application points.

## 3. The residual stiffness analysis

The stiffness analysis is based on the moment-curvature response of the pure bending zone. The monitoring scheme enables the curvature estimation in different ways: from vertical displacements of LVDT  $L_1$ – $L_9$  and from surface deformations identified using the LVDT  $L_{10}$ – $L_{15}$  or DIC system. References (Kaklauskas et al., 2011; Kaklauskas & Gribniak, 2016; Gribniak et al., 2017) describe the data processing algorithms. Analysis of the alternative curvature values enables avoiding errors due to measurement interruptions or other inaccuracies.

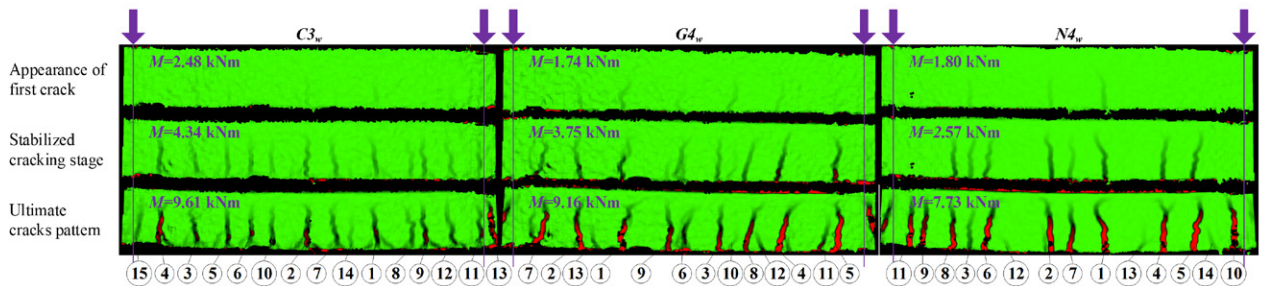


Figure 2. Cracking schemes identified by the DIC system

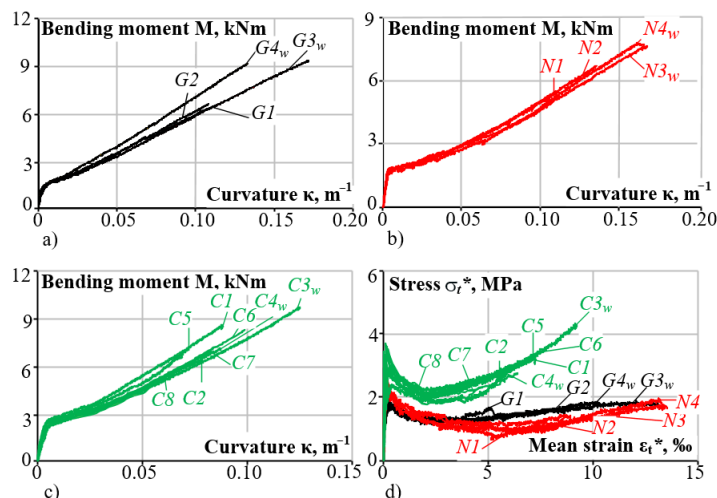


Figure 3. Moment-curvature diagrams of different beam groups: a) internal GFRP bars; b) NSM strips; c) EBR systems; and d) the equivalent residual stresses in the tensile concrete  $\sigma_t^*$  of the beams

Figure 3 shows the moment-curvature diagrams constructed using the surface deformations captured by the DIC system. The differences between the diagrams of nominally identical specimens could be related with variation in the cross-section dimensions. The corresponding equivalent stiffness models are shown in Figure 3d. As can be observed, the diagrams of the nominally identical specimens are practically coincident. Analysis of the residual stiffness models reveals significant efficiency of the external CFRP reinforcement system concerning the internal reinforcing schemes. This effect is the object of further research.

The diagrams shown in Figure 3d were derived using the proposed concept of the average stress of tensile concrete. It implies the following assumptions: smeared crack approach; linear strain distribution within the section depth; elastic behaviour of reinforcement and compressive concrete; rectangular distribution of stresses in the tensile concrete. The latter assumption enables a closed-form analytical solution of the residual stiffness problem. Figure 4 illustrates the assumed model. Based on the equilibrium equations of internal forces and bending moments in respect to the centroid of the equivalent tensile stress diagram, the equivalent average stress in the tensile concrete and the corresponding strain can be expressed as

$$\sigma_t^* = \kappa \frac{y_c^2 b E_c - 2(d - y_c) E_s A_s}{2(h - y_c)b}, \quad \varepsilon_t^* = \kappa \frac{h - y_c}{2}, \quad (1)$$

where  $E_c$  and  $E_s$  are the elasticity moduli of concrete and reinforcement;  $A_s$  is the reinforcement area; other notations are evident from Figure 4a. Position of the neutral axis is estimated as

$$y_c = \frac{1}{3C_3} \left\{ 2\bar{C} \cos \left( \frac{1}{3} \cos^{-1} \left\{ -\frac{27C_3^2 C_0 - 9C_3 C_2 C_1 + 2C_2^3}{2\bar{C}^3} \right\} \right) - C_2 \right\},$$

$$\bar{C} = \sqrt{C_2^2 - 3C_3 C_1}. \quad (2)$$

Using the following coefficients

$$C_3 = \frac{\kappa E_c b}{12}, \quad C_2 = \frac{\kappa}{4} (2E_s A_s + E_c b h), \quad C_1 = \frac{\kappa E_s A_s}{4} (h - 3d),$$

$$C_0 = \frac{\kappa d^2 E_s A_s}{2} \left( 2 - \frac{h}{d} \right) - M_{ext}. \quad (3)$$

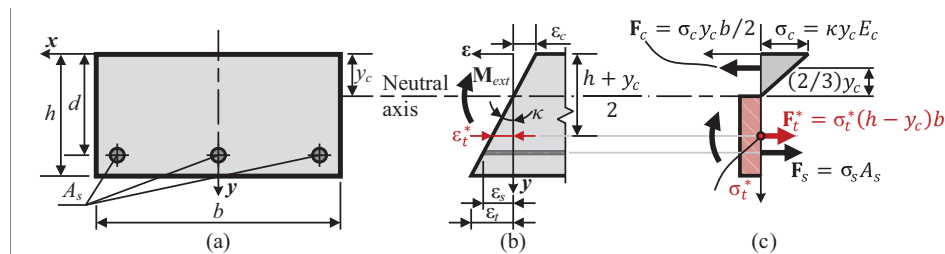


Figure 4. Analytical model of the element subjected to external bending moment  $M_{ext}$ : a) RC section; b) strain profile; c) stresses and internal forces acting in section

Analysis of the residual strength models (expressed in term of the equivalent stresses  $\sigma_t^*$ ) reveals a noticeable efficiency of the external CFRP reinforcement system concerning the internal reinforcing schemes. The area under the equivalent stress diagram determine the deformation energy related to the relative contribution of the cracked concrete.

## Conclusions

Efficiency of different composite reinforcement schemes was analysed experimentally: 16 beam specimens reinforced either with internal GFRP bars, near-surface mounted (NSM) CFRP strips, or externally bonded (EBR) CFRP sheets were tested. The residual stiffness determines the efficiency of the reinforcement. An analytical model, representing a closed-form solution of the residual stiffness problem in flexural members, was proposed. The external CFRP sheets demonstrated the most efficient resistance of the concrete cracking among the considered reinforcement systems. In essence, the decay of the residual equivalent stresses acting in the tensile concrete does not exceed 50% of the tensile strength of the concrete in the presence of the EBR system. This effect is the object of further research.

## Acknowledgements

Prof L. Torres would like to acknowledge the support of Spanish Government (MINECO), project Ref. BIA2017-84975-C2-2-P.

## Author contributions

HAS, AR, and AS were responsible for data collection and analysis. Together with AS, HAS wrote the first draft of the article. AR and AS were responsible for data interpretation. VG and LT conceived the study and were responsible for the design and development of the data analysis. VG also made the final proofread.

## Disclosure statement

The authors declare that they have not any competing financial, professional, or personal interests from other parties.

## References

- Gribniak, V., Kaklauskas, G., Juozapaitis, A., Kliukas, R., & Meskenas, A. (2017). Efficient technique for constitutive analysis of reinforced concrete flexural members. *Inverse Problems in Science and Engineering*, 25(1), 27–40. <https://doi.org/10.1080/17415977.2015.1135139>
- Gribniak, V., Sokolov, A., Rimkus, A., Sultani, H. A., Tunçay, M. C., & Torres, L. (2019, March 20–22). A novel approach to residual stiffness of flexural concrete elements with composite reinforcement. In *Proceedings of the IABSE Symposium – Towards a Resilient Built Environment Risk and Asset Management*, Rovinj, Croatia.
- Kaklauskas, G., & Ghaboussi, J. (2001). Stress-strain relations for cracked tensile concrete from RC beam tests. *ASCE Journal of Structural Engineering*, 127(1), 64–73. [https://doi.org/10.1061/\(ASCE\)0733-9445\(2001\)127:1\(64\)](https://doi.org/10.1061/(ASCE)0733-9445(2001)127:1(64))
- Kaklauskas, G., & Gribniak, V. (2016). Hybrid tension stiffening approach for decoupling shrinkage effect in cracked reinforced concrete members. *ASCE Journal of Engineering Mechanics*, 142(11), 04016085. [https://doi.org/10.1061/\(ASCE\)EM.1943-7889.0001148](https://doi.org/10.1061/(ASCE)EM.1943-7889.0001148)
- Kaklauskas, G., Gribniak, V., Salys, D., Sokolov, A., & Meskenas, A. (2011). Tension-stiffening model attributed to tensile reinforcement for concrete flexural members. *Procedia Engineering*, 14, 1433–1438. <https://doi.org/10.1016/j.proeng.2011.07.180>
- Torres, L., Barris, C., Kaklauskas, G., & Gribniak, V. (2015). Modelling of tension-stiffening in bending RC elements based on equivalent stiffness of the rebar. *Structural Engineering and Mechanics*, 53(5), 997–1016. <https://doi.org/10.12989/sem.2015.53.5.997>
- Torres, L., López-Almansa, F., & Bozzo, L. (2004). Tension-stiffening model for cracked flexural concrete members. *ASCE Journal of Structural Engineering*, 130(8), 1242–1251. [https://doi.org/10.1061/\(ASCE\)0733-9445\(2004\)130:8\(1242\)](https://doi.org/10.1061/(ASCE)0733-9445(2004)130:8(1242))
- SKIRTINGOMIS KOMPOZITINĖMIS SISTEMOMIS ARMUOTŲ BETONINIŲ ELEMENTŲ LENKIAMOJO STANDUMO LYGINAMOJI ANALIZĖ**
- H. A. Sultani, V. Gribniak, A. Rimkus, A. Sokolov, L. Torres**
- Santrauka
- Betono konstrukcijoms armuoti naudojamos įvairios medžiagos ir technologijos, tačiau unifikuotos metodikos, kuria būtų galima palyginti skirtingų armavimo sistemų mechanines savybes, nėra. Konstrukcinės sistemos armavimo efektyvumas gali būti vertinamas atsižvelgiant į elementų liekamąjį standumą. Šiame straipsnyje pateikiamas supaprastintas lenkiamojo standumo analizės metodas. Jis apima naują bandymų schemą, kuria siekiama gauti tolygų plyšių pasiskirstymą mažame laboratoriniame bandinyje. Siūlomas analitinis sprendimas nereikalauja nei iteracinio skaičiavimo, nei detalaus apkrovos istorijos aprašymo. Nagrinėjamos kelios kompozitinio armavimo sistemos: taikant stiklo pluoštu armuotus polimerinius (GFRP) strypus, išdėstytus elemento viduje, anglies pluoštu armuotus polimerinius (CFRP) lakštus, priklijuotus elemento išorėje, ir sijų paviršiuje tvirtinamas anglies pluoštu armuotas polimerines (NSM) juostas. Tyrimo rezultatai rodo anglies pluoštu armuotų polimerų (CFRP) sistemų, išdėstytų elementų išorėje, efektyvumą.
- Reikšminiai žodžiai:** betono kompozitas, armavimas, liekamasis standumas, analitinis modelis, lenkimo bandymai.